Original Article

A Study on Clinical Characteristics and Magnetic Resonance Imaging Manifestations on Systemic Rosai-Dorfman Disease

Xiao Cheng, Jing-Liang Cheng, An-Kang Gao

Department of Magnetic Resonance Imaging, The First Affiliated Hospital of Zhengzhou University, Zhengzhou, Henan 450000, China

Abstract

Background: Rosai-Dorfman disease (RDD) is typically characterized by painless bilateral and symmetrical cervical lymphadenopathy, with associated fever and leukocytosis. The aim of the current study was to summarize the clinical features and imaging characteristics of RDD, in an effort to improve its diagnostic accuracy.

Methods: The study was analyzed from 32 patients between January 2011 and December 2017; of these, 16 patients had pathologically diagnosed RDD, eight had pathologically diagnosed meningioma, and eight pathologically diagnosed lymphoma. All patients underwent computed tomography and magnetic resonance imaging (MRI). Clinical features and imaging characteristics of RDD were analyzed retrospectively. The mean apparent diffusion coefficient (ADC) values of lesions at different sites were measured, and one-way analysis of variance and the least significant difference *t*-test were used to compare the differences between groups and draw receiver operating characteristic curves. The tumors were excised for biopsy and analyzed using immunohistochemistry.

Results: The mean ADCs were $(0.81 \pm 0.10) \times 10^{-3}$ mm^2/s for intercranial RDD, $(0.73 \pm 0.05) \times 10^{-3}$ mm^2/s for nasopharyngeal RDD, $(0.74 \pm 0.11) \times 10^{-3}$ mm^2/s for bone RDD, and $(0.71 \pm 0.04) \times 10^{-3}$ mm^2/s for soft-tissue RDD. The optimum ADC to distinguish intracranial RDD from lymphoma was 0.79×10^{-3} mm^2/s (62.5% sensitivity and 100% specificity) and to distinguish meningioma from intracranial RDD was 0.92×10^{-3} mm^2/s (62.5% sensitivity and 100% specificity). Levels of C-reactive protein, erythrocyte sediment rate and D-dimer were significantly elevated (81%, 87%, and 75%, respectively). On immunohistochemistry, RDD was positive for both S-100 and CD68 proteins but negative for CD1a.

Conclusions: Conventional MRI, combined with diffusion-weighted imaging and ADC mapping, is an important diagnostic tool in evaluating RDD patients. An accurate diagnosis of RDD should consider the clinical features, imaging characteristics, and the pathological findings.

Key words: Apparent Diffusion Coefficient; Clinical Feature; Imaging Manifestation; Magnetic Resonance Imaging; Rosai-Dorfman Disease

Introduction

Rosai-Dorfman disease (RDD) is a rare form idiopathic non-Langerhans cell histiocytosis, also known as sinus histiocytosis with massive lymphadenopathy. RDD clinically manifests as painless, massive cervical lymphadenopathy, with associated fever, weight loss, and polyclonal hypergammaglobulinemia. Although originally described as a nodal disorder, extranodal disease has occurred in up to 40% of cases, with disease sites including the skin, central nervous system, upper respiratory tract, orbit and eyelid, and gastrointestinal tract.[1] This rare disease demonstrates predominance in young adults, although cases in older adult have been documented.

Access this article online

Quick Response Code:

Website: www.cmj.org

DOI: 10.4103/0366-6999.225053

The etiology and pathogenesis of RDD are currently unknown, and the disease can easily be misdiagnosed. In this study, we analyzed 16 cases of RDD confirmed by pathology, summarized the patients' clinical and imaging features, and reviewed the relevant literatures. The aim of this study was to

Address for correspondence: Dr. Jing-Liang Cheng, Department of Magnetic Resonance Imaging, The First Affiliated Hospital of Zhengzhou University, 1 Jianshe Road, Zhengzhou, Henan 450000, China
E-Mail: cjr.chjl@vip.163.com

Received: 16-10-2017 **Edited by:** Peng Lyu

How to cite this article: Cheng X, Cheng JL, Gao AK. A Study on Clinical Characteristics and Magnetic Resonance Imaging Manifestations on Systemic Rosai-Dorfman Disease. Chin Med J 2018;131:440-7.

use clinical and imaging features to improve the diagnostic accuracy of RDD.

Methods

Ethical approval

The study was conducted in accordance with the *Declaration of Helsinki* and was approved by the Ethical Committee of The First Affiliated Hospital of Zhengzhou University. All patients gave informed consent for the present study.

Study population

We retrospectively analyzed the medical records of 32 patients who were treated with definitive surgery at our hospital from January 2011 to December 2017. Of these, 16 patients had pathologically diagnosed RDD, eight patients with pathologically diagnosed meningioma, and eight patients with pathologically diagnosed lymphoma which were located in brain. All patients underwent surgery for total or subtotal resection of tumors. None of the patients underwent radio- or chemo-therapy postoperatively. Patients were followed up after the surgery between 1 and 24 months.

Imaging scanning

All patients underwent computed tomography (CT, Discovery, 750HD, General Electric Company, America) and magnetic resonance imaging (MRI, 3.0T magnetic resonance scanner, Skyro, Siemens, Germany) scanning with the fast low angle shot 2D sequence T1-weighted (repetition time [TR] 250ms, echo time [TE] 2.5 ms) in the sagittal plane and cross-sectional scanning; and the turbo spin echo (SE) sequence T2-weighted imaging (TR 4500 ms, TE 100 ms) in the cross-sectional plane, a layer thickness 5 mm, no spacing interval, and two excitation imaging. On axial diffusion-weighted imaging (DWI), a SE echo planar imaging sequence was used with TR 3700 ms and TE 102 ms, b-values of 0 and 1000, a layer thickness of 5 mm, layer spacing 1.8 mm, and a matrix field of view of 219 mm × 219 mm. The apparent diffusion coefficient (ADC) map was generated automatically. During enhanced scanning, patients were injected with contrast agent (gadopentetate dimeglumine [Beijing Beilu Pharmaceutical Co., China]) at a dose of 0.2 ml/kg.

Image analysis

To obtain ADC values, multiple small circular regions of interest (ROIs) measuring 10–20 voxels (7–15 mm^2) were manually delineated on the pretreatment ADC map that was created using Syngo workstation (Siemens, Germany). All ROIs were drawn by radiologists blinded to patient outcomes and corresponded to T2-weighted, enhanced T1-weighted, and DWI images. Radiologists meticulously avoided areas of cystic change, necrosis, or hemorrhage and selecting the mean ADC at the maximum level of the lesion, took measurements three times, and calculated the mean value of three ADCs.

Pathological examination

Erythrocyte sediment rate (ESR), C-reactive protein (CRP), and D-dimer levels were assayed in all patients. Postoperative specimens were stained with hematoxylin and eosin and immunohistochemical staining to detect antibodies for CD1a, S-100 protein, and CD68.

Statistical analysis

SPSS 20.0 (IBM Corporation Inc., Armonk, NY, USA) was used for statistical analysis. ADC values were expressed as means ± standard deviations (SD). If the data were in normal distributions, comparisons were assessed with the Student's *t*-test between intracranial and other parts RDD. One-way analysis of variance (ANOVA) was used to compare differences between the mean ADC values for intracranial RDD, meningioma, and lymphoma. A value of $P < 0.05$ was considered statistically significant. The least significant difference *t*-test was also used to compare between the two groups and a receiver operating characteristic (ROC) curve was drawn. The Youden index ([sensitivity + specificity] −1) estimated threshold value of ADC values.

Results

Clinical and laboratory examination

The 16 participants included eight women and eight men who were aged between 1 and 63 years (mean age, 37.9 ± 20.6 years). Of the 16 patients, five cases of lesions located in the cerebrum and three in the cerebellum, which manifested as headache and dizziness. Of four cases were located in the nasopharynx and neck, which mainly manifested as progressive painless swelling. Of one case was located in the thigh bone, two case was located in the ribs, and one case was located in the hip, which mainly manifested as pains of the lesion. After surgery and during the follow-up period, lesions recurred in one patient. Clinical data of the 16 patients are summarized in Table 1. The levels of CRP were significantly elevated (33.78 ± 46.44 mg/L) in 13 patients (81%) and the ESR elevated (34.44 ± 26.18 mm/h) in 14 patients (87%). Furthermore, D-dimer levels were slightly elevated (0.56 ± 0.65 μg/ml) in 12 patients (75%).

Neuroimaging results

Of the intracranial lesions [patient 2, Figure 1] of patients 1–8, CT imaging showed that the lesions had a slightly hyperdense and a nonuniform enhancement. MRI revealed a heterogeneous T1-weighted signal, and a hyperintensity mixed with hypointensity signal on T2-weighted images. In addition, edema was detected around the lesions and manifested as hypointensity within an area of hyperintensity on the T2 dark fluid sequence. DWI showed that lesions were diffusion limited. There was heterogeneous enhancement of lesions on dynamic contrast enhancement imaging.

For the lesions located in the nasopharynx and neck of patients 9–12, CT imaging indicated that the lesions were soft-tissue masses. The boundaries of the lesions were not clearly delineated on CT imaging and the lesions showed nonuniform signal enhancement. MRI showed that

Table 1: Clinical characteristics of patients with RDD

Patient	Gender	Age (years)	Location	Clinical presentation	Preoperative diagnosis	Treatment	Follow-up (months)
1	Female	41	Left temporal lobe	Headache Dizziness Nausea	Glioma	Resection	8
2	Female	63	Left cerebellum and cerebellar vermis	Apsychia Nausea	Intracerebral hemorrhage	Evacuation of cerebellar hematoma	7
3	Male	10	Left temporal lobe	Nausea Headache	Meningoma	Resection	5
4	Female	35	Left frontal lobe	Apsychia Nausea	Meningoma	Resection	8
5	Female	20	Right temporal lobe	Headache Dizziness	Meningoma	Resection	6
6	Male	37	Left temporal lobe	Apsychia Headache Weakness in the limbs	Lymphoma	Resection	6
7	Male	60	Cerebellum	Headache Nausea	Meningoma	Resection	3
8	Male	59	Right cerebellum	Headache Weakness in the limbs	Lymphoma	Paracentesis	2
9	Male	55	Right nasopharynx and bilateral neck	Toothache	Lymphoma or Castleman disease	Resection	24
10	Female	26	Nasopharynx and neck	Nasal obstruction	Polypus	Resection	24
11	Male	8	Pharynx and neck	Nasal obstruction	RDD	Resection	24
12	Female	47	Nasopharynx and neck	Fever	Lymphoma	Paracentesis	18
13	Male	1	Thigh bone	Fever	Osteosarcoma	Paracentesis	24
14	Female	59	Rib	Chest pain	Thoracic neoplasm	Resection	9
15	Female	29	Sternum and rib	Chest pain	Thoracic neoplasm	Resection	12
16	Male	57	Hip	Pain	Infection	Resection	13

RDD: Rosai-Dorfman disease.

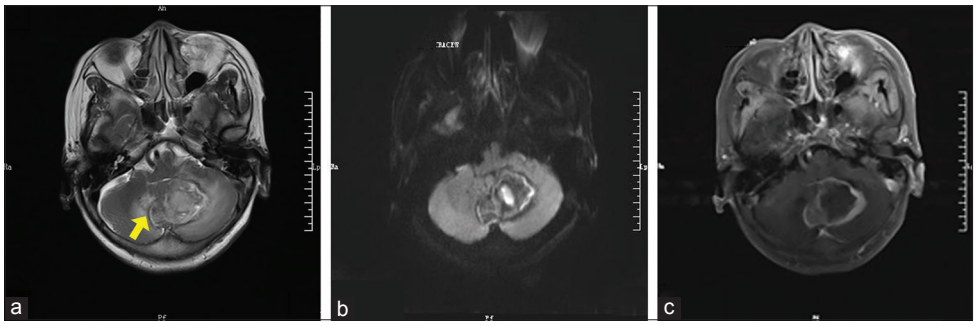

Figure 1: Representative imaging findings of a 63-year-old woman (patient 2): (a) T2-weighted showed the lesion was located in the left cerebellum and cerebellar vermis (arrow). There was a hyperintensity mixed with hypointensity, which heterogeneous signal on T2 weighted. There was mild edema surrounding the mass. (b) The lesion is diffusion-limited on the DWI scan. (c) The lesion was heterogeneously enhanced, following administration of the contrast agent. DWI: Diffusion-weighted imaging.

these lesions had hyperintensity on T1-weighted, and a hyperintensity mixed with hypointensity on T2-weighted, nonuniform enhancement, and the bone adjacent to the nasopharynx was not destroyed [patient 9, Figure 2].

For lesions located in the bone of patients 13–15, soft-tissue lesions were found adjacent to bones of patients 13–15. CT imaging showed isodense or hyperdense soft-tissue masses, with associated osteolytic

destruction. On CT contrast enhancement, the lesion showed slightly irregular in homogeneous enhancement. MRI revealed multiple bone lesions with hypointensity on T1- and hyperintensity on T2-weighted images and with strong enhancement after injection of gadolinium contrast agent.

For the lesions located in the hip of patient 16, MRI showed the lesions as irregular and cystic, with a heterogeneous hyperintensity on T1- and T2-weighted. On fat-suppression T1 sequence, the lesions showed high signal. DWI revealed the lesions to be diffusion restricted. On dynamic contrast enhancement, the capsule wall of the lesion showed slight reinforcement, with no reinforcement of the cystic cavity [patient 16, Figure 3].

The mean ADC value of intracranial RDD was $(0.81 \pm 0.10) \times 10^{-3}$ mm^2/s. Within the head, malignant lymphomas had a mean ADC value of $(0.61 \pm 0.12) \times 10^{-3}$ mm^2 and meningomas was $(0.94 \pm 0.11) \times 10^{-3}$ mm^2. A ROC curve was drawn based on the mean ADC value of patients [Figure 4]. The optimum ADC to distinguish meningoma from

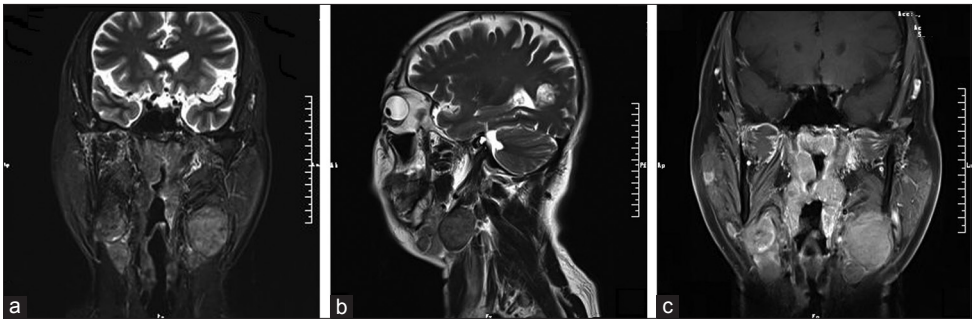

Figure 2: Imaging findings of a 55-year-old man (patient 9): (a) T2-weighted coronal and (b) T2-weighted sagittal MRI scans showed the lesion was located in the right nasopharynx and bilateral neck. There was no edema surrounding the mass. (c) The lesion was homogeneously enhanced, following administration of the contrast agent. MRI: Magnetic resonance imaging.

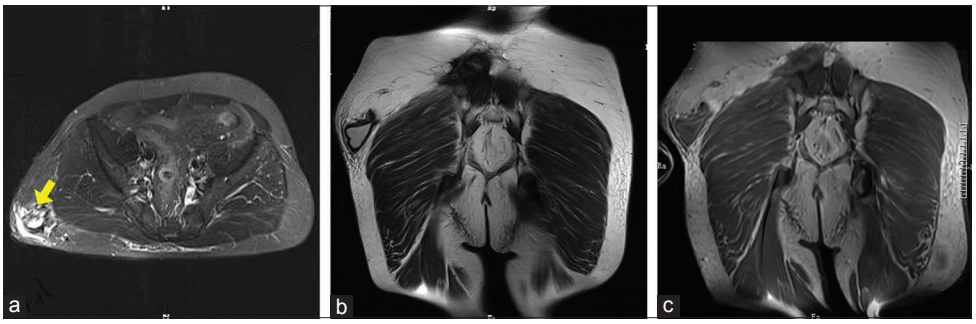

Figure 3: Imaging findings of a 57-year-old man (patient 16). (a) T2-weighted axial (arrow) and (b) T2-weighted coronal MRI scans showed the lesion was located in the subcutaneous soft tissue of the hip. (c) The cystic wall of the lesion was slightly enhanced, following administration of the contrast agent. MRI: Magnetic resonance imaging.

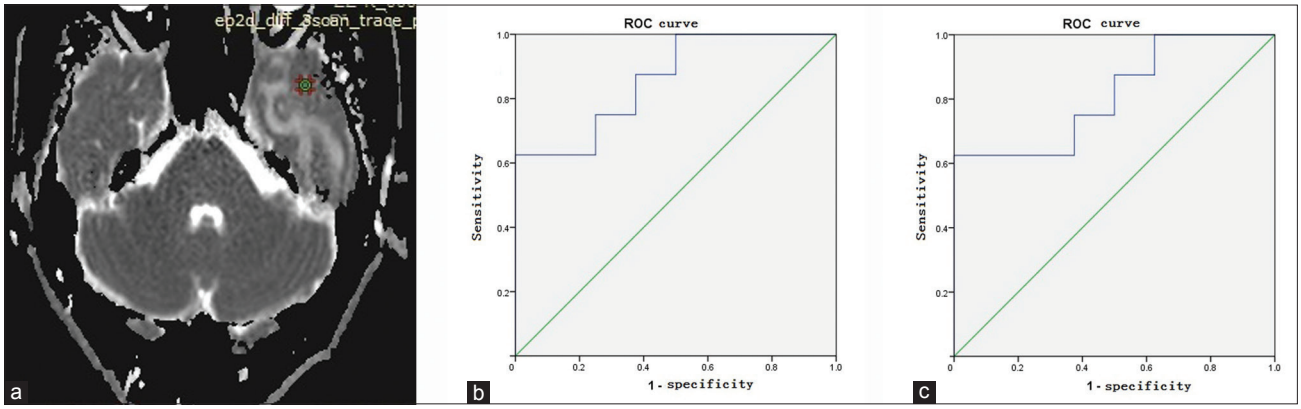

Figure 4: Select the ROI and measure the ADC value on ADC map. (a) The ADC map of patient 6. The green circle is the select area. (b) The ROC curve of ADC value between intracranial RDD and malignant lymphomas. The area under the ROC curve was 0.859. The optimum ADC was 0.79×10^{-3} mm^2/s (62.5% sensitivity and 100% specificity). (c) The ROC curve of ADC value between meningoma and intracranial RDD. The area under the ROC curve was 0.813. The optimum ADC was 0.92×10^{-3} mm^2/s (62.5% sensitivity and 100% specificity). ROI: Region of interest; ADC: Apparent diffusion coefficient; ROC: Receiver operating characteristic curve; RDD: Rosai-Dorfman disease.

intracranial RDD was 0.92×10^{-3} mm^2/s (62.5% sensitivity and 100% specificity), and the area under the ROC curve (AUROC) was 0.813. The optimum ADC to distinguish intracranial RDD from malignant lymphomas was 0.79×10^{-3} mm^2/s (62.5% sensitivity and 100% specificity), and the AUROC was 0.859. The mean ADC values of RDD located in nasopharynx and neck, bone, and soft tissue were $(0.73 \pm 0.05) \times 10^{-3}$ mm^2/s, $(0.74 \pm 0.11) \times 10^{-3}$ mm^2/s, and $(0.71 \pm 0.04) \times 10^{-3}$ mm^2/s, respectively. There is no difference between the ADC values of intracranial RDD and other parts RDD [Table 2].

Pathological findings

Patients underwent excisional biopsy followed by pathological examination of excised tissue. Tissue samples were grayish-red or grayish-yellow in appearance and contained large, pale histiocytes with vacuolated eosinophilic cytoplasm, mixed with scattered plasma cells, and mature lymphocytes. Emperipolesis, consisting of histiocytes engulfed in well-preserved lymphocytes, was observed in the permanent paraffin-embedded tissues [patient 4, Figure 5]. Immunohistochemical analysis showed that the masses were positive for S-100 and CD68 proteins but negative on CD1a staining.

Follow-up and outcomes

None of the patients underwent chemotherapy or radiotherapy after surgery. During the follow-up period, with the exception of one patient who had a recurrence of RDD, all other patients were symptom-free, with no disease progression identified on either CT imaging or MRI.

Discussion

Overview of Rosai-Dorfman disease

RDD is an extremely rare nonmalignant histiocytic disorder. Usually, patients present with painless swollen cervical lymph nodes. Extranodal involvement is common and may occur in more than 40% of patients, sometimes without associated lymphadenopathy.[2] The most frequent affected extranodal sites include the skin and soft tissue (17%); the nasal cavity and paranasal sinuses (16%); the eye, orbit, and ocular adnexa (11%); the bone (11%); the salivary gland (7%); the central nervous system (7%); the oral cavity (4%); the kidney and genitourinary tract (3%); the respiratory tract (3%); the liver (1%); the tonsil (1%); the breast (<1%); the gastrointestinal tract (<1%); and the heart (<1%).[3,4] RDD is usually more common in children and adolescents although RDD located in the skin and intracranial is more common in middle-aged and elderly people. Only three of the 16 cases in this study occurred in adolescents, the median age of patients was 37.94 ± 20.56 years. The precise causative mechanism of RDD remains unknown, but immune system dyscrasias and viral infections, specifically human herpesvirus 6, have been implicated in the previous study.[5] Moreover, current evidence suggested a possible role for SLC29A3 mutations in familial RDD.[6]

Imaging manifestations of Rosai-Dorfman disease

In this article, we have summarized the clinical and imaging features of RDD lesions located in the head, neck, bone, and hip. Intracranial RDD usually occurs without extracranial lymphadenopathy, and most intracranial lesions are attached to the dura such as the convex surface of the brain, the saddle area, the middle cranial cavity, the sagittal, and the cavernous sinus, with only few cases extending into the parenchyma. Common signs include cephalgia, seizure, weakness of limbs, and cranial nerve deficiency, depending on the location of the lesion. Intracranial RDD is usually visualized as a mixed isointense or hyperintense mass on T1-weighted MRI, with distinct borders and heterogeneous contrast enhancement. On T2-weighted images, the lesions usually presented heterogeneous hyperintense signals and sometimes hypointense signals.[7] Some studies have postulated that the aggregation of hypointense signals on T2-weighted images is a characteristic manifestation

Table 2: The ADC values of RDD, meningioma, and lymphoma

Group	*n*	Mean ADC ($\times 10^{-3}$ mm^2/s)	Statistics	*P*
Intracranial RDD	8	0.81 ± 0.10	16.560*	0.001
Meningoma	8	0.94 ± 0.11		
Lymphoma	8	0.61 ± 0.12		
RDD (nasopharyngeal, bone, soft tissue)	8	0.74 ± 0.07	1.645†	0.122‡

*F = 16.560; One-way ANOVA was used to compare differences between the mean ADC values for intracranial RDD, meningioma, and lymphoma, P = 0.001; LSD-T was used to compare between groups; The ADC of intracranial RDD was statistically significant compared with meningiomas, P = 0.029. The mean ADC of RDD was statistically significant compared with lymphomas, P = 0.003. The ADC of meningiomas was statistically significant compared with lymphomas, P = 0.001. †t = 1.645; Comparisons were assessed with the Student's t-test between intracranial and other parts RDD. ‡The ADC of intracranial RDD was no statistically significant compared with RDD located in other parts, P = 0.122. ANOVA: Analysis of variance; ADC: Apparent diffusion coefficient; RDD: Rosai-Dorfman disease; LSD-T: Least significant difference t-test.

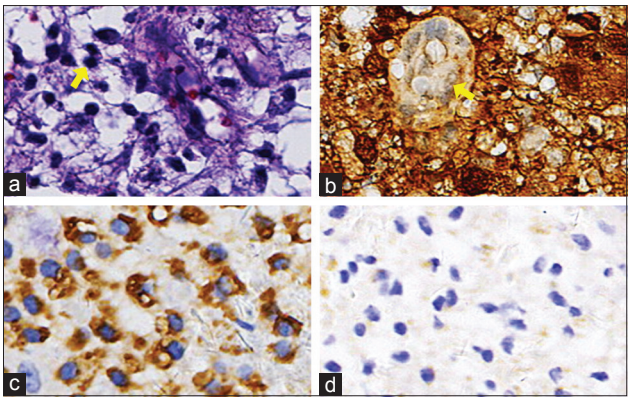

Figure 5: Histopathological manifestations of patient 4. (a) Hematoxylin and eosin-stained section demonstrating an area of lymphocyte engulfment by a lesional histiocyte consistent with emperipolesis (arrow, original magnification ×400). (b) Immunohistochemical labeling for S-100 protein was diffusely positive within the lesional histiocytes (original magnification ×400). (c) Immunohistological finding: Some histiocytes showed CD68 protein was positive (original magnification ×400). (d) Immunohistochemical labeling for CD1a protein was negative within the lesional histiocytes (original magnification ×400).

of RDD and may be related to free radicals released by macrophages during phagocytosis.[8,9] However, in the study, only one patient presented with aggregation of hypointense signals on T2-weighted images, and lesions usually had minimal contrast enhancement.[10] Meningiomas usually have an isointense signal on T1-weighted MRI, a hypointense signal on T2-weighted MRI, and homogeneous enhancement on dynamic contrast enhancement images. In this study, intracranial lesions had a slightly high density and nonuniform enhancement on CT imaging. In addition, the presentation on MRI was consistent with that in previous studies. Magnetic resonance spectroscopy (MRS) has particular specificity for some patients. In meningiomas, the proton spectrum indicated that the alanine spectrum was significantly elevated, and its peak was 48 ppm, while in intracranial RDD, the spectrum indicated that the choline peak was 140 ppm, which can distinguish from meningioma.[11] Therefore, MRI combined with MRS might be a useful method of diagnosing RDD and meningiomas.

The lesions of four patients were located in the nasopharynx, which is the disease site with the second highest occurrence rate of extranodal RDD. Nasopharyngeal RDD was mostly located in the maxillary sinus.[12] RDD located in nasal cavity and nasopharynx manifest as diffuse mucosa thickening and invades the nasal dorsum and subcutaneous tissues. Moreover, this type of RDD can also manifest as polypoid and soft-tissue masses, along with invasion and deterioration of sclerotin, or as a proliferating cirrhosis of the sinusoidal wall. These lesions typically showed uneven enhancement on dynamic contrast enhancement scans.[13] In the present finding, four nasopharyngeal RDD were of the soft-tissue type, which showed a uniform density on CT and MRI scans and did not invade the sclerotin of the nasopharynx, which were consistent with previous studies. Nasopharyngeal RDD needs to be distinguished from nasal polyps and squamous cell carcinoma of the nasopharynx. Nasal polyps are usually located in the middle nasal meatus, and enhanced MRI scans show a manifestation in the polyp mucosa, which are often obscured by the bone around the nasopharynx. Squamous cell carcinoma of the nasopharynx is an invasive growth, with nonuniform density and necrosis commonly found in the cervical lymph nodes. In addition, imaging manifestations combined with laboratory and pathological examination might be helpful for diagnosing RDD.

Bone involvement is a rare manifestation of RDD occurring in approximately 10% of RDD cases and with a balanced sex distribution. Wei *et al*.[14] have reported that bone RDD is often located in bones including the long bones, craninal bones, fingers, and phalanges. Bone lesions in RDD are primarily osteolytic on conventional radiographic imaging, with some lesions also showing sclerotic margins. Symptoms typically include pain and swelling. In this study, three patients presented with RDD in bone. CT showed osteolytic changes in these three patients, consistent with descriptions in the literature. Bone RDD is usually misdiagnosed as chronic, nonspecific inflammatory changes, tuberculosis, or other cancers and relies on postoperative pathological examination for the correct diagnosis.

Soft-tissue RDD (STRDD) is rare, with sporadic cases previously reported in no more than 3% of RDD patients. The female : male ratio of STRDD cases is approximately 3:1. STRDD is also characterized by a broad tumor size range and a wide patient age range.[15] A study by Al-Daraji *et al*.[15] reported that multifocal STRDD was much more prone to recurrence. There is no difference in STRDD recurrence rates between men and women, possibly due to low incidence of the disease. We identified one patient with STRDD; this patient had an isolated mass on the hip but no signs of recurrence during 13 months of follow-up. Imaging examinations such as CT and MRI were useful for evaluating the extent of STRDD, although there were no specific characteristics.[16]

DWI is an MRI technique based on measuring water diffusion in tissues. This diffusion can be quantified by ADC. According to the literature, ADC values can be used to discriminate between malignant and benign lesions; typically, malignant tumors have lower values than benign lesions.[17] RDD shows high signal-restricted diffusion on DWI. In this study, malignant lymphomas in the head had a mean ADC value of $(0.61 \pm 0.12) \times 10^{-3}$ mm^2/s and meningomas of $(0.94 \pm 0.11) \times 10^{-3}$ mm^2/s, while intracranial RDD had a mean ADC value of $(0.81 \pm 0.10) \times 10^{-3}$ mm^2/s. In this report, the mean ADC values of RDD located in nasopharyngeal, bone, and soft tissue were $(0.73 \pm 0.05) \times 10^{-3}$ mm^2/s, $(0.74 \pm 0.11) \times 10^{-3}$ mm^2/s, $(0.71 \pm 0.04) \times 10^{-3}$ mm^2/s, respectively. The ADC value of intracranial RDD was no statistically significant compared with RDD located in other parts (nasopharyngeal, bone, and soft tissue). The ADC value is associated with several histopathological features. It has been shown that there is an inverse correlation between the ADC and cell count of lesions.[18] The mean ADC value of intracranial RDD was higher than that of lymphomas but lower than that of meningiomas in the study, possibly due to the cellular structure of RDD. The mechanism of RDD might involve infiltration of small neoplastic cells, such as those of malignant lymphomas, which disrupt the movement of water molecules, resulting in vasogenic edema, destruction of brain tissue, or infiltration of large cells. Microscopic examination of RDD lesions reveals plasma cells, lymphocytes, and large histiocytes within a dense collagenous background. On histopathological examination, plasma cells are numerous, often arranged along small blood vessels. This might explain the low ADC values of RDD. In conclusion, conventional MRI combined with DWI might help to determine the activity of RDD and to evaluate patients with the disease.

Histopathology of Rosai-Dorfman disease

Diagnosis of RDD is usually confirmed on pathological examination. Noguchi *et al*.[15] reported that some patients with RDD had a slight elevated of CRP and ESR; in addition, there may be nonspecific increases in other laboratory parameters in cases of RDD, according to another study.[19] However, in this study, we found that D-dimer

levels increased in twelve patients. Specimens are typically obtained by an open surgical biopsy or fine-needle aspiration. In general, histopathological analysis shows a large number of mixed-cell populations, including mature plasma cells and lymphocytes.[1] The most commonly detected cells are histiocytes with an accentuated phagocytic appearance. The infiltration of these inflammatory cells might be related to the increase in D-dimer levels. These histiocytes harbor apparently intact lymphocytes, lending the appearance of a "cell within a cell," or emperipolesis.[20] Emperipolesis is not a unique phenomenon to RDD and has been seen in both normal and leukemic processes.[1] On immunohistochemical staining, RDD histiocytes were positive for CD68, CD14, HLA-DR, fascin, CD163, and S-100, but typically negative for CD1a, enabling the disease to be distinguishing from Langerhans histiocytosis. The differential diagnosis of RDD includes histiocytosis of Langerhans cells, histiocytic sarcoma, lysosomal storage diseases (e.g., Gaucher disease), classical Hodgkin lymphoma, melanoma and metastatic carcinomas, and infections involving the lymph nodes caused by histoplasma and mycobacteria. Pathology and laboratory examinations are an effective means of distinguishing RDD from other diseases.[9]

Treatment of Rosai-Dorfman disease

Most patients with RDD experience a chronic disease course. Due to its low incidence, no optimal or standard treatment has been defined. The disease is often self-limiting with a very good outcome; nevertheless, 5–11% of patients die from this disease. Treatment strategies can vary according to the severity of vital organ involvement. Primarily, patients undergo surgery or receive glucocorticoids. Systemic corticosteroids are usually helpful in decreasing nodal size and symptoms; however, they can be immunosuppressive, with possible RDD recurrence after a short period of interruption. Chemotherapy for the treatment of RDD has shown controversial results. Methotrexate and 6-mercaptopurine have shown potential for efficacy and requires further investigation.[5] Another report have suggested using alpha-interferon, although its side effects have limited its use.[21] Anti-CD20 monoclonal antibody/rituximab has been described in one case.[22] In addition to chemotherapy, the role of radiotherapy for RDD is not well understood. Some reports have described a full resolution of RDD with treatment by radiotherapy, whereas others have shown no response.[23]

We analyzed 16 cases of RDD confirmed by pathology, and summarized the patients' clinical and imaging features. ESR, CRP, and D-dimer of RDD patients were increased. Only one patient of RDD manifested the aggregation of hypointense within hyperintense on T2-weighted. RDD showed high signal and diffusion restricted on DWI; a low ADC value. The ADC value is useful for distinguishing intracranial RDD, meningioma, and lymphoma. Conventional MRI combined with DWI might help to determine the activity of disease and to evaluate patients with RDD. However, this study had some limitations. The sample size was small, particularly for patients with nasopharyngeal, bone, and STRDD. Further studies with larger samples are therefore needed. In conclusion, the accurate diagnosis of RDD should consider the clinical features, imaging characteristics, and the pathological findings.

Financial support and sponsorship

Nil.

Conflicts of interest

There are no conflicts of interest.

References

1. Chen YP, Jiang XN, Lu JP, Zhang H, Li XQ, Chen G, *et al.* Clinicopathologic analysis of extranodal Rosai-Dorfman disease of breast: A report of 12 cases (in Chinese). Chin J Pathol 2016;45:556-60. doi: 10.3760/cma.j.issn.0529-5807.2016.08.012.
2. Rodriguez-Galindo C, Helton KJ, Sánchez ND, Rieman M, Jeng M, Wang W, *et al.* Extranodal Rosai-Dorfman disease in children. J Pediatr Hematol Oncol 2004;26:19-24. doi: 10.1097/00043426-200401000-00007.
3. Dalia S, Sagatys E, Sokol L, Kubal T. Rosai-Dorfman disease: Tumor biology, clinical features, pathology, and treatment. Cancer Control 2014;21:322-7. doi: 10.1177/107327481402100408.
4. Shi SS, Sun YT, Guo L. Rosai-Dorfman disease of lung: A case report and review of the literatures. Chin Med J 2009;122:873-4. doi: 10.3760/cmaj.issn.0366-6999.2009.97.020.
5. O'Malley DP, Duong A, Barry TS, Chen S, Hibbard MK, Ferry JA, *et al.* Co-occurrence of Langerhans cell histiocytosis and Rosai-Dorfman disease: Possible relationship of two histiocytic disorders in rare cases. Mod Pathol 2010;23:1616-23. doi: 10.1038/modpathol.2010.157.
6. Morgan NV, Morris MR, Cangul H, Gleeson D, Straatman-Iwanowska A, Davies N, *et al.* Mutations in SLC29A3, encoding an equilibrative nucleoside transporter ENT3, cause a familial histiocytosis syndrome (Faisalabad histiocytosis) and familial Rosai-Dorfman disease. PLoS Genet 2010;6:e1000833. doi: 10.1371/journal.pgen.1000833.
7. Di Rocco F, Garnett MR, Puget S, Pueyerredon F, Roujeau T, Jaubert F, *et al.* Cerebral localization of Rosai-Dorfman disease in a child. Case report. J Neurosurg 2007;107:147-51. doi: 10.3171/PED-07/08/147.
8. Toh CH, Chen YL, Wong HF, Wei KC, Ng SH, Wan YL, *et al.* Rosai-Dorfman disease with dural sinus invasion. Report of two cases. J Neurosurg 2005;102:550-4. doi: 10.3171/jns.2005.102.3.0550.
9. Zhu H, Qiu LH, Dou YF, Wu JS, Zhong P, Jiang CC, *et al.* Imaging characteristics of Rosai-Dorfman disease in the central nervous system. Eur J Radiol 2012;81:1265-72. doi: 10.1016/j.ejrad.2011.03.006.
10. Wu M, Anderson AE, Kahn LB. A report of intracranial Rosai-Dorfman disease with literature review. Ann Diagn Pathol 2001;5:96-102. doi: 10.1053/adpa.2001.23027.
11. Yue Q, Isobe T, Shibata Y, Anno I, Kawamura H, Yamamoto Y, *et al.* New observations concerning the interpretation of magnetic resonance spectroscopy of meningioma. Eur Radiol 2008;18:2901-11. doi: 10.1007/s00330-008-1079-6.
12. La Barge DV 3rd, Salzman KL, Harnsberger HR, Ginsberg LE, Hamilton BE, Wiggins RH 3rd, *et al.* Sinus histiocytosis with massive lymphadenopathy (Rosai-Dorfman disease): Imaging manifestations in the head and neck. AJR Am J Roentgenol 2008;191:W299-306. doi: 10.2214/AJR.08.1114.
13. Shi XY, Ma DL, Fang K. Cutaneous Rosai-Dorfman disease presenting as a granulomatous rosacea-like rashs. Chin Med J 2011;124:793-4. doi: 10.3760/cma.j.issn.0366-6999.2011.05.031.
14. Wei J, Zhang Y, Jin J, Zhang J. Cutaneous Rosai-Dorfman disease accompanied by Langerhans cell hyperplasia responsive to combined treatment. Chin Med J 2014;127:3200. doi: 10.3760/cma.jissn.0366-6999.20141123.
15. Al-DarajiW, Anandana A, Klassen-Fischer M, Auerbach A,

Marwahaa J, Fanburg-Smith J. Soft tissue Rosai-Dorfman disease: 29 new lesions in 18 patients, with detection of polyomavirus antigen in 3 abdominal cases. Ann Diagn Pathol 2010;14:309-16. doi: 10.1016/j.anndiagpath.
16. Akyigit A, Akyol H, Sakallioglu O, Polat C, Keles E, Alatas O, *et al.* Rosai-Dorfman disease originating from nasal septal mucosa. Case Rep Otolaryngol 2015;2015:232898. doi: 10.1155/2015/232898.
17. Padhani AR, Liu G, Koh DM, Chenevert TL, Thoeny HC, Takahara T, *et al.* Diffusion-weighted magnetic resonance imaging as a cancer biomarker: Consensus and recommendations. Neoplasia 2009;11:102-25. doi: 10.1593/neo.81328.
18. Surov A, Meyer HJ, Wienke A. Correlation between apparent diffusion coefficient (ADC) and cellularity is different in several tumors: A meta-analysis. Oncotarget 2017;8:59492-9. doi: 10.18632/oncotarget.17752.
19. Romero Arenas MA, Singhi AD, Hruban RH, Cameron AM. Rosai-Dorfman disease (sinus histiocytosis with massive lymphadenopathy) of the pancreas: Third reported occurrence. J Gastrointest Cancer 2012;43:626-9. doi: 10.1007/s12029-012-9424-z.
20. Shi Y, Griffin AC, Zhang PJ, Palmer JN, Gupta P. Sinus histiocytosis with massive lymphadenopathy (Rosai-Dorfman disease): A case report and review of 49 cases with fine needle aspiration cytology. Cytojournal 2011;8:3. doi: 10.4103/1742-6413.76731.
21. Kidd DP, Revesz T, Miller NR. Rosai-Dorfman disease presenting with widespread intracranial and spinal cord involvement. Neurology 2006;67:1551-5. doi: 10.1212/01.wnl.0000242893.55416.
22. Scheel MM, Rady PL, Tyring SK, Pandya AG. Sinus histiocytosis with massive lymphadenopathy: Presentation as giant granuloma annulare and detection of human herpesvirus 6. J Am Acad Dermatol 1997;37:643-6. doi: 10.1016/S0190-9622(97)70186-5.
23. Cooper SL, Chavis PS, Fortney JA, Watkins JM, Caplan MJ, Jenrette JM 3rd, *et al.* A case of orbital Rosai-Dorfman disease responding to radiotherapy. J Pediatr Hematol Oncol 2008;30:744-8. doi: 10.1097/MPH.0b013e31817e4ac1.

Rosai-dorfamn病的临床表现及影像学研究

摘要

背景: Rosai-Dorfman病(RDD)是以无痛, 对称性, 双侧颈淋巴结增生为典型表现的疾病, 常伴随发热和白细胞增多。 本研究总结了16例RDD的临床病理和影像学特征, 以提高诊断的准确性。

方法: 回顾分析了2011年1月至2017年12月就诊于我院的32名患者, 术后免疫组化及病理证实16例为RDD, 8例为脑膜瘤, 8例为淋巴瘤, 分析RDD的临床及影像特征。 患者均进行了CT及MRI扫描, 测量不同部位疾病的 表观弥散系数 (ADC)值, 使用单因素方差分析比较各组均值, LSD-*t*检验比较两两差异, 受试者工作特征 (ROC)曲线预测最佳阈值。

结果: 颅内RDD的平均ADC值是 $(0.81 \pm 0.10) \times 10^{-3}$ mm^2/s, 鼻咽部RDD的平均ADC值是 $(0.73 \pm 0.05) \times 10^{-3} mm^2/s$,骨RDD的平均ADC值是 $(0.74 \pm 0.11) \times 10^{-3}$ mm^2/s, 软组织RDD的平均ADC值是 $(0.71 \pm 0.04) \times 10^{-3}$ mm^2/s。 区别颅内RDD与淋巴瘤的最佳ADC阈值是 0.79×10^{-3} mm^2/s (62.5% 敏感性, 100%特异性), 区别颅内RDD与脑膜瘤的最佳ADC阈值是0.92×10^{-3} mm^2/s (62.5%敏感性, 100%特异性)。 RDD的C-反应蛋白, 血沉和D-二聚体都显著升高 (分别为81%, 87%和75%)。 RDD免疫组化结果表现为S-100 和 CD68为阳性, 而CD1a为阴性。

结论: 传统MRI, 结合弥散加权成像(DWI)及ADC值, 可以作为评估RDD患者的重要方法。 RDD的准确诊断需考虑临床特征, 影像特征及病理结果。